WELDING RESEARCH

SUPPLEMENT TO THE *WELDING JOURNAL*, APRIL 1999
Sponsored by the American Welding Society and the Welding Research Council

Modeling and Analysis of Laser Melting within a Narrow Groove Weld Joint

Experimental melt patterns on 304 stainless steel agree well with calculation and simulation results

BY J. O. MILEWSKI AND M. B. BARBE

ABSTRACT. The reflective propagation and absorption of laser energy within a narrow metal root opening has been modeled using a computer-based optical design program to predict the location of melting. A three-dimensional ray tracing model considers the effect of laser parameters, joint geometry and material reflectivity to predict the location of energy absorption and the onset of melting. Focal spot location changes and F number changes, corresponding to a matrix of experimental conditions, are used as input to a series of simulation runs. Experimental data are used to define the location of the onset of melting in 304 stainless steel and to verify the energy density threshold of melting predicted from simulation results. Melt patterns, produced by single Nd:YAG laser pulses, on the joint groove faces are analyzed and compare well with calculation and simulation results. The results of this study provide quantitative experimental validation of this model that can be used to understand and apply fundamental principals of nonimaging optics for enhanced laser processing.

Introduction

The reflective propagation of light into a V-shaped groove and the concentration of this energy was shown by Mendenhall in 1911 (Ref. 1). The reflective propagation of laser energy to transport energy deep within a weld joint has been demonstrated in various industrial applications (Refs. 2–5). To fully apply the physics of nonimaging optics to laser processing of materials, we must first understand the interaction and contribution of the pertinent system parameters beginning with the simplest, most well understood effects. For this understanding to be of practical value, it must be represented in a model that can provide ease of simulation for scientists and engineers to use on a case-by-case basis using readily available computer resources.

Previous modeling of the energy transport due to multiple internal reflections has focused primarily on the understanding of laser keyhole mode melting, cutting and drilling processes (Refs. 6–9). We are developing a model to help understand laser energy propagation and concentration within various narrow groove joint geometries and have experimentally verified the enhanced melting of various metals, including aluminum.

It is useful to compare melting produced by energy trapping within a narrow joint opening to conduction mode and keyhole mode melting. Conduction mode melting generally displays a low depth-to-width aspect ratio weld and is generally a stable mode of melting. It suffers from low coupling efficiency where as much as 90% or more of the impinging beam energy is lost due to reflection of the beam off the surface of the weld pool. Keyhole mode melting is generally characterized by a transition from energy densities required for melting to those producing melting and vaporization of the metal to be welded. The resultant vapor cavity can trap the laser beam and increase coupling efficiencies to well over 50%. The requirements for high-powered lasers to achieve and maintain the vapor cavity, coupled with the inherent unstable dynamic balance between vapor cavity pressure and surface tension, make this melting mode difficult to control particularly for partial penetration welds.

KEY WORDS

Laser Welding
Melt Model
Reflectivity
Joint Geometry
Nonimaging Optics
Narrow Groove
Stainless Steel

We have been shown that under certain conditions (Refs. 3–5) the effect of beam energy trapping can enhance the melting within a narrow groove joint. Joint geometry, such as a narrow V groove, and laser optical conditions, such as focal position and F number, can be used to transport the laser energy deep within the weld joint to produce high aspect ratio welds. These high aspect ratio welds can be produced without the requirement to exceed conduction mode melting conditions. High aspect ratio multipass welds in stainless steel and aluminum have been produced by this method. Increased laser efficiency and process stability has been demonstrated. This method in effect uses the principles of nonimaging optics and extends the optical design of the system to include the weld joint.

A two-dimensional geometrical op-

J. O. MILEWSKI and M. B. BARBE are with Los Alamos National Laboratory, Los Alamos, N.Mex.

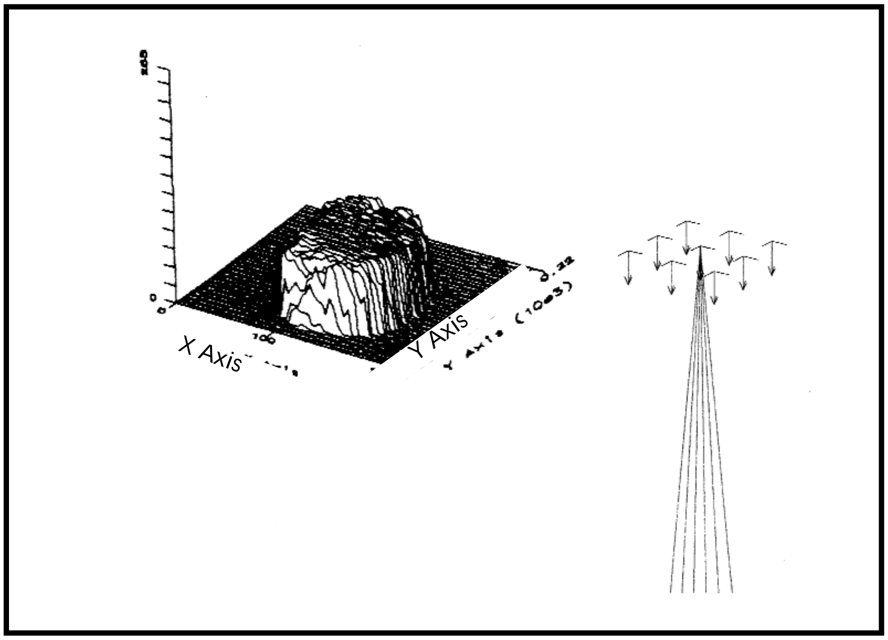

Fig. 1 — The two-dimensional point source array shown on the right is used for the representation of the "top hat" laser spatial intensity profile, at the focal spot, shown on the left.

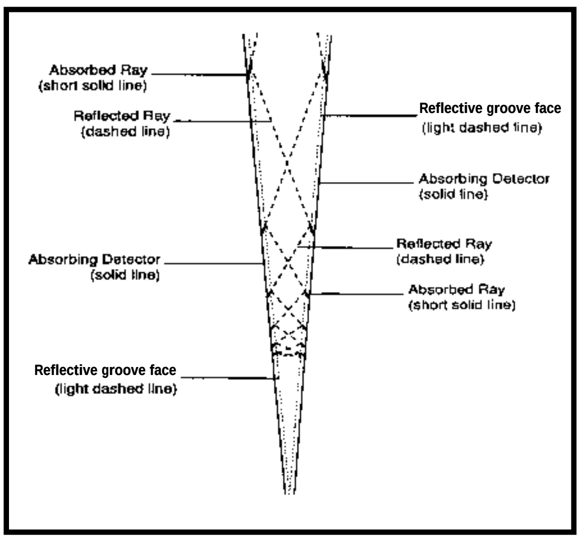

Fig. 2 — The propagation of a single ray into a simulation of a V-joint cross section shows increased frequency of reflections and increased incident angle as a function of depth in the joint. Partially reflective groove faces are backed up with a detector array, that records the location of energy absorption.

tics model has been used to predict the location of energy absorption within a weld joint due to primary reflections (Refs. 10, 11) using ray tracing. Experimental results showed enhanced melting due to energy trapping and improvements in the depth-to-width aspect ratio of the resultant welds. Qualitative comparison between simulated peak energy locations and experimental weld locations showed good correspondence. The two-dimensional model previously constructed has been extended to the three-dimensional case (Ref. 12). In this study, quantitative prediction of the location and intensity of absorbed energy for laser spot welds were made considering only specular reflections and constant absorption as a function of ray incident angle. Comparison with experimental data was made to evaluate the usefulness for validation and refinement of this simplified model and is the purpose of this investigation. A longer-term objective of this research is to validate a series of simple process models, which may be used by welding engineers to evaluate and optimize the design of laser joints.

Description of the Model

A three-dimensional model was constructed to represent laser energy propagation into a linear narrow groove V joint. The laser beam is represented by a two-dimensional distribution of point sources spatially distributed to approximate the extent of the focal spot of the laser beam as shown in Fig. 1. Rays emanate from these point sources over a solid angle defined by the F number of the laser beam being modeled. They carry with them directional information and a unit of energy defined by

$$\varepsilon_{r0} = E_i / (n_r * n_p) \qquad (1)$$

where E_i is the energy of the laser pulse in joules, n_r is the number of rays and n_p is the number of point sources.

The rays are directed into the joint root opening defined by two partially reflective surfaces in the model. As a ray strikes the surface, part of the energy is reflected, as defined by a constant reflection coefficient, and the other part is absorbed at that location, as shown in Fig. 2. The spatial frequency and incident angle of reflections are seen to increase with depth within the V joint. This demonstrates the energy concentration of this nonimaging optical system. Within the model, the energy passing through the surface is absorbed by a two-dimensional array of fully absorbing elements. The element absorbing the energy $a_{(x,y)}$ defines the location of energy absorption. The energy absorbed within the surface element after each absorption event is described by the following relationship:

$$\varepsilon_{ap} = \varepsilon_{ap} + (\varepsilon_{rn} * \alpha) \qquad (2)$$

where ε_{ap} is the previous amount of energy stored in that element, α is the coefficient of absorption and ε_{rn} is the energy in the ray after n reflections.

The propagation of the ray is halted when

$$\varepsilon_{rn} < \varepsilon_{r0} * 0.01. \qquad (3)$$

The model allows geometric rendering of the input conditions as shown in Fig. 3 and plotting of energy intensity as a function of location within the weld joint, as shown in Fig. 4. A constant coupling coefficient is used to approximate the absorption of Nd:YAG laser energy by the material irrespective of incident angle. No other angle-dependent effects, such as polarization, or temperature-dependent effects are considered in this simplified model.

Description of Experiment

An experimental matrix was constructed using the parameters described in Table 1. A V groove was machined into samples of 304 stainless steel. The samples were clamped and positioned beneath the laser beam. Three sets of five spot welds each were made, each set

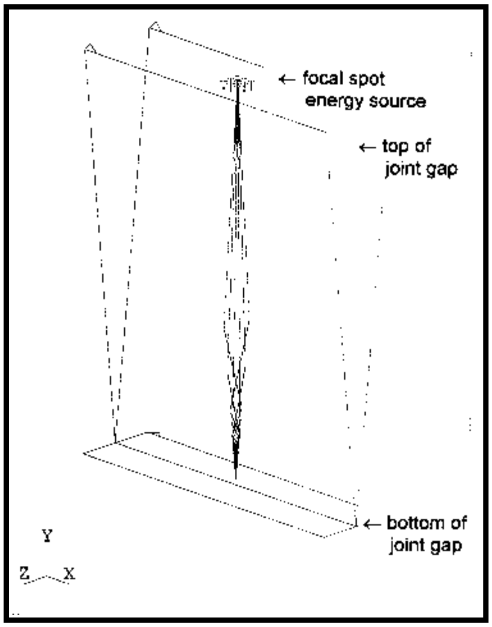

Fig. 3 — A three-dimensional rendering, produced by the optical CAD model, allows visualization of the geometric optical conditions and the joint geometry. A few rays, emanating from a single point source, are shown to illustrate energy propagation into the narrow groove joint.

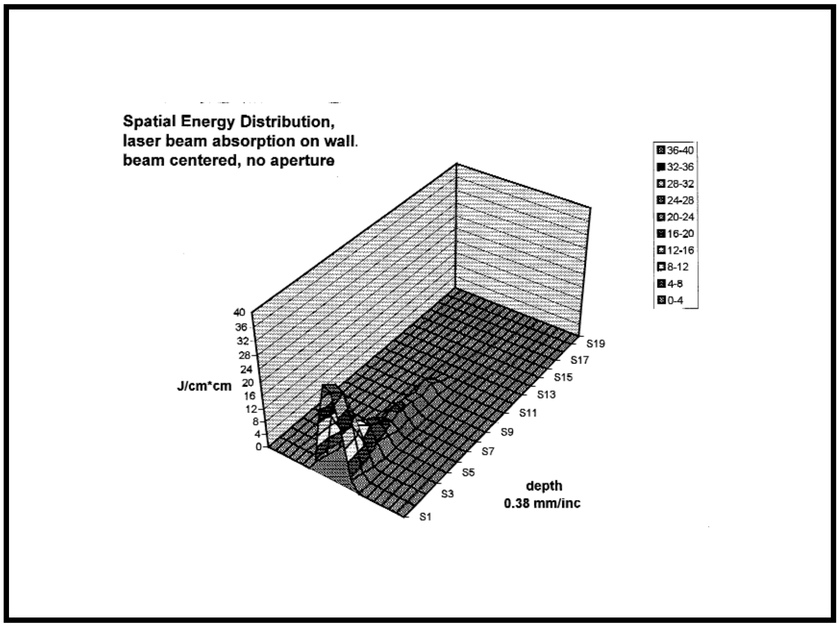

Fig. 4 — A graphical output showing the predicted location and intensity of absorbed energy is useful to understand where the energy is absorbed within the weld joint. An energy absorption peak is located at the joint bottom.

using either no beam aperture or beam apertures of 4.3 or 2.54 mm and varying focal spot locations offset in height and transverse to the weld joint centerline. These changes varied the F number, spot size and relative position of the laser beam with respect to the narrow groove. Resultant groove face melt patterns were analyzed by breaking apart the samples, photographing and measuring the extent of melting as a function of parameter changes. The location and shape of the groove face melt patterns were used for comparison with the model simulation results produced using the same input conditions. The F number was calculated by the use of burn patterns of the beam prior to final focusing and kapton burn spot measurements of the final focal point diameters for the various aperture beams. The average power was measured using a laser beam power meter prior to entering the final focal lens. Laser lamp power was adjusted to achieve a constant output power of 100 W for each aperture series of tests.

Simulation Conditions

The input conditions to the model were changed to simulate all 15 conditions of the experimental weld matrix. A constant coupling coefficient of 0.3 was used to approximate the coupling

Table 1 — Experimental Parameters Used in the Study

Experimental Parameters, Constant			
laser model	Raytheon SS-500		
laser type	pulsed Nd:YAG		
focal length	100 mm		
laser power delivered	100 W		
pulse length	7 ms		
number of pulses	1		
joint depth	7.6 mm		
joint type equal	12-deg included angle		
joint fixture	clamped		
cleaning used	degrease/electro-polish		
cover gas	argon		
material, 304 SS	Alloy 304 stainless steel		
Experimental Parameters, Varied			
Experiment Series	Series 1	Series 2	Series 3
beam aperture	none	4.3 mm	2.54 mm
focal spot size	0.48 mm	0.40 mm	0.33 mm
F number	F6.4	F7.26	F8.88
Sample 1, 6, 11	0 offset, surface focus	0 offset, surface focus	0 offset, surface focus
Sample 2, 7, 12	0 offset, focus +1 mm	0 offset, focus +1 mm	0 offset, focus +1 mm
Sample 3, 8, 13	0 offset, focus –1 mm	0 offset, focus –1 mm	0 offset, focus –1 mm
Sample 4, 9, 14	–0.5-mm offset, surface focus	–0.5-mm offset, surface focus	–0.5 mm offset, surface focus
Sample 5, 10, 15	–1-mm offset, surface focus	–1-mm offset, surface focus	–1-mm offset, surface focus

Parameters show three identical series of focal depth and offset changes, as a function of three beam aperture conditions.

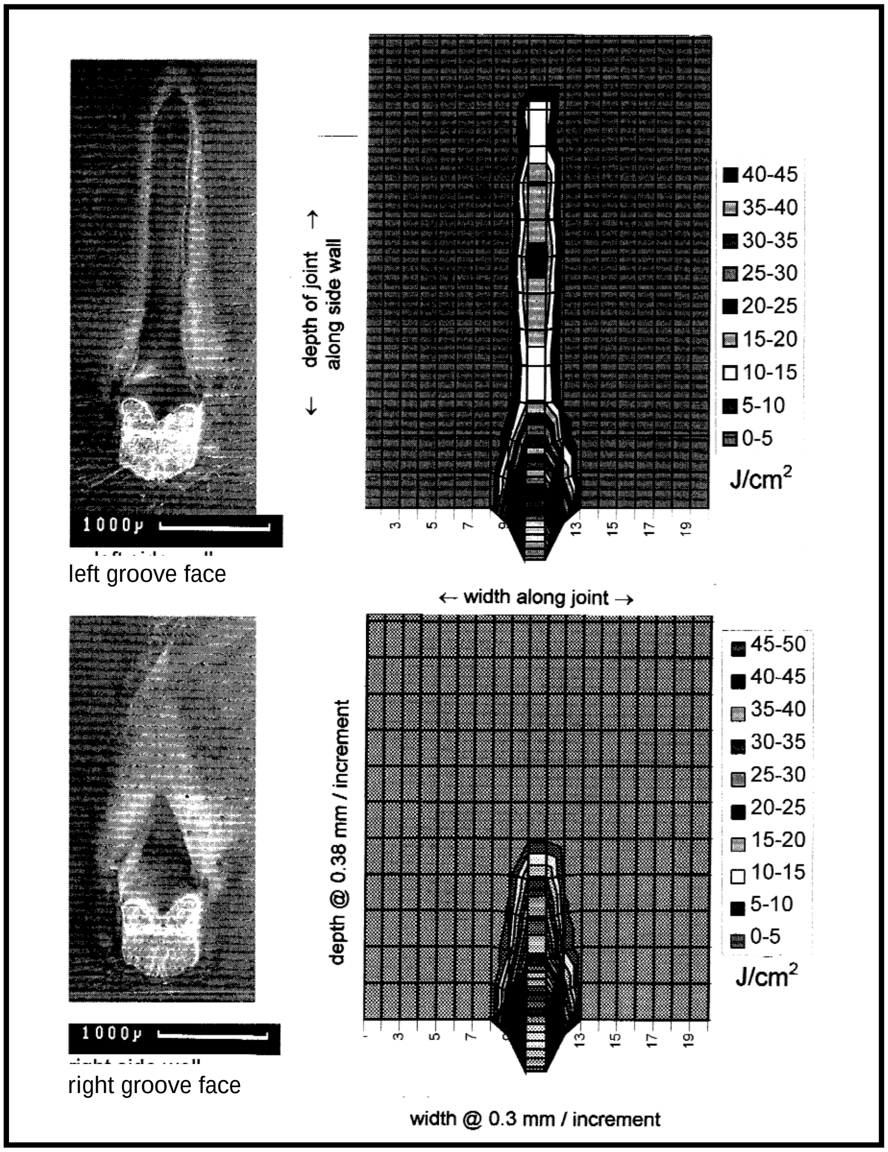

Fig. 5 — A qualitative comparison of the groove face melt profiles observed in an experiment, where the beam is offset toward the left groove face, compares well to the prediction energy absorbed as simulated under the same conditions.

Table 2 — Melting Threshold Data

Simulation id No.		F No.	Range of Peak Intensity, J/cm² (simulation)	Range of Melting Thresholds Indexed to Experiment J/cm²	Average Melting Threshold for Series J/cm²
1–5	Series 1	F6.4	24–38	8–13	10
6–10	Series 2	F7.2	30–48	4–6	5
10–15	Series 3	F8.8	44–64	5–7	6

Data was derived by comparing the boundary of the experimental melt regions with the energy plots obtained from the corresponding simulation data.

of the Nd:YAG wavelength to stainless steel (Ref. 13). Other input parameters included beam spot size, focal point location, weld joint geometry, detector array size and laser energy in joules. Nine thousand rays, distributed over nine point sources, and oriented at each point over a solid angle defined by the F number of the laser beam, as previously determined by experimental measurement, were traced. The location of energy absorption was recorded within a matrix of cells distributed along the walls of the simulated weld joint. The model is constructed using the OptiCad geometrical optical design software and was run under the Windows 95® operating system on a 200-MHz Pentium-based PC. The model took approximately 5 min to nonsequentially trace all of the rays within this V-joint geometry. Plotting of the spatial energy distribution allowed analysis of the shape and intensity of the simulated laser beam propagation. Planar contours of energy per unit area were rendered using this method of analysis, enabling comparison with experiments.

Calculation of the enthalpy of melting of 304 stainless steel was approximated using the following relationship:

$$\Delta H = m[(Cp*\Delta T) + \Delta H_f] \quad (4)$$

where a density of 7.9 g/cm^2 was assumed for stainless steel, heat capacity, Cp, 502 J/(kg*K), and heat of fusion, H_f, 2.5 * 105 J/kg.

Solving for an assumed volume 1 cm^2*0.125 mm thickness, we calculate an energy threshold of 7 J/cm^2 required to melt stainless steel. This energy density number was used to compare with the predicted energy intensity contours corresponding to the indexing of experimental-to-simulation data.

Experimental Results

The V-groove joint was broken apart to reveal groove face melting patterns with a characteristic teardrop shape. The shape of these patterns varied considerably as a function of the experimental input parameters. The use of beam apertures produced smaller spot sizes and larger F numbers. Spot welds produced using larger F-number conditions resulted in longer, narrower melt patterns. Offset of the laser focal spot toward one groove face created a preferential melting of that groove face higher in the weld joint but similar melting on either side toward the joint root. Focusing the laser deeper into the weld joint created a corresponding larger melt region at the weld root. A misalignment of the beam with respect to the weld joint for the third series of tests by 0.05 mm was accommodated in the simulation studies by an additional offset within the model input parameters. Images of the extent of the fusion boundary melting were scaled for direct comparison with simulation output graphs as shown in Fig. 5. As an example, a condition of beam offset produced a disjoint melted region high in the weld joint root opening corresponding to an energy peak predicted from the simulation of that case, as shown in Fig. 6.

Comparison with Simulation Results

A comparison between actual melt profiles and simulation profiles was qualitatively very good. There was good correlation between the melt boundaries and iso-energy intensity profiles from the model within each of the three data sets, but the correlation was less between data sets associated with different aperture conditions. Table 2 shows the three simulation series (1–5, 6–10, 11–15) indexed to the corresponding experimental series. The actual experimental melt regions are compared with simulations to determine the energy density predicted by melting to the corresponding melt boundary. Average values of the best fit melting thresholds were calculated for each data series. These values were compared to the approximate melting threshold indicated by the enthalpy of melting calculation. These average values were used as a basis to directly compare melt height and width of simulation vs. the experiment in Figs. 7–9. Melt region widths compared most favorably with simulation. The melt regions' heights compared less closely, though these were within a few J/cm^2 within a single series of runs. Peak energy intensities of between 24 and 62 J/cm^2 were predicted by the model over

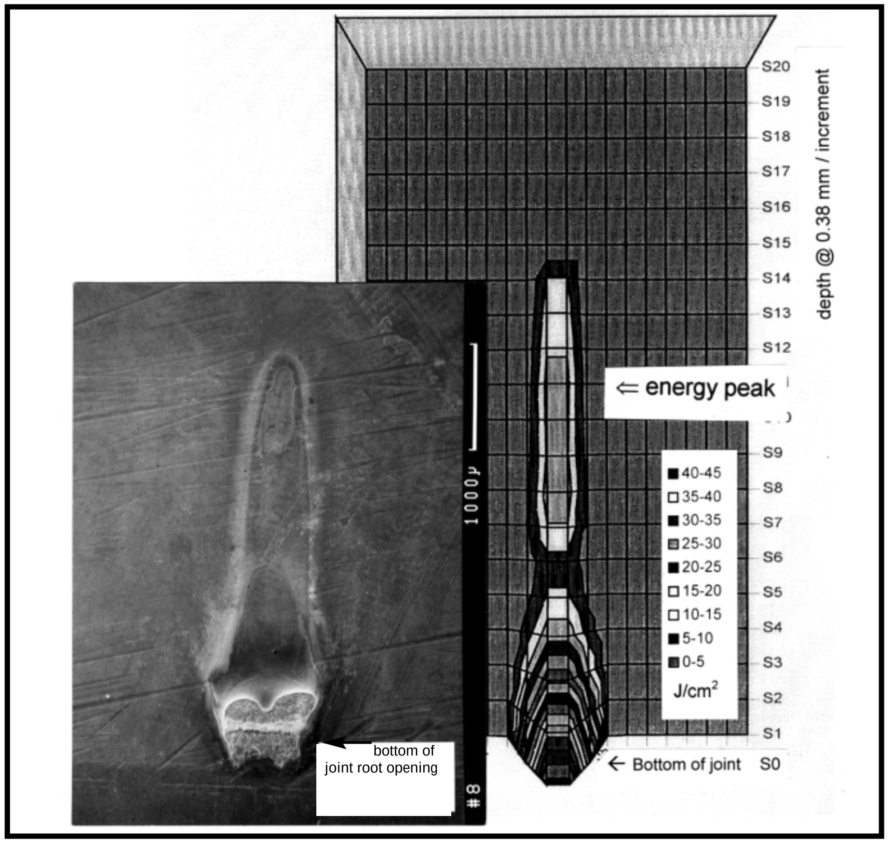

Fig. 6 — Beam offset produced melting high in the joint and corresponds to an energy peak in a simulation made using the same conditions.

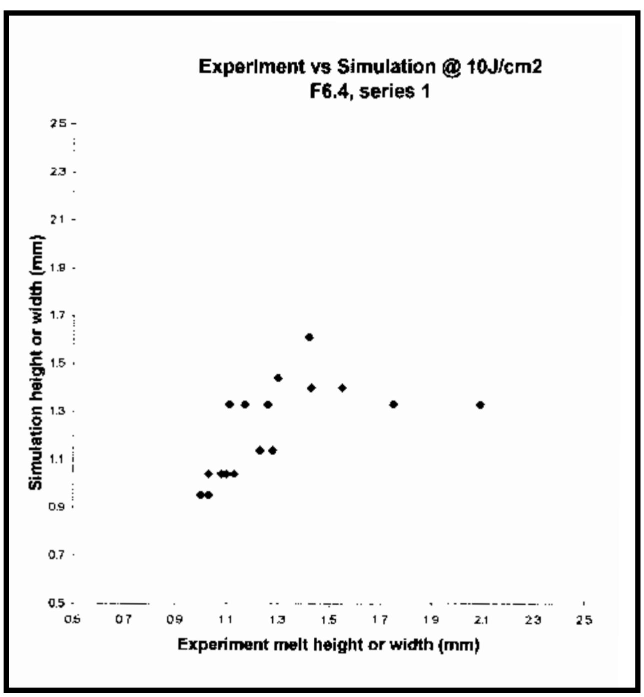

Fig. 7 — Experiment melt region height and width measurements vs. simulation height and width data for the F6.4 series, indexed at a calculated melting threshold of 10 J/cm^2.

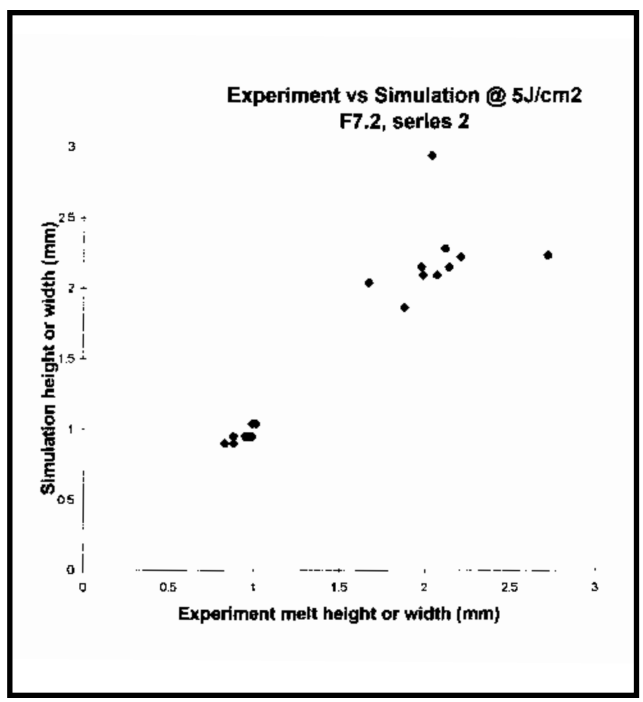

Fig. 8 — Experiment melt region height and width measurements vs. simulation height and width data for the F7.2 series, indexed at a calculated melting threshold of 5 J/cm^2.

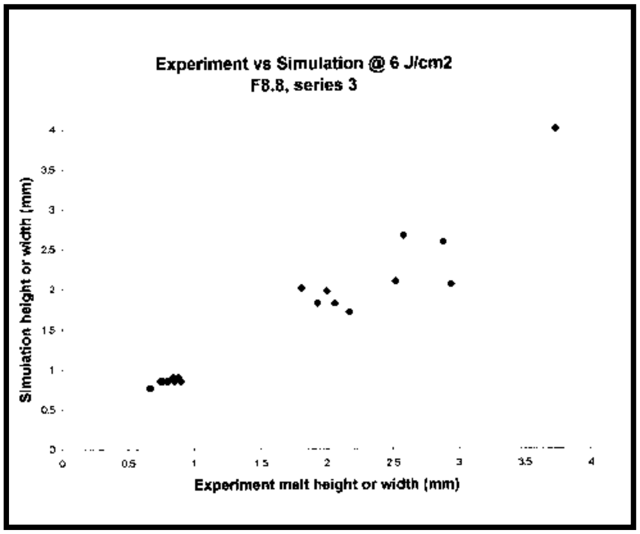

Fig. 9 — Experiment melt region height and width measurements vs. simulation height and width data for the F8.8 series, indexed at a calculated melting threshold of 6 J/cm².

the entire set of simulations. The difference between the average melting energy threshold between the data sets was 5 J/cm^2 or approximately 8% of the range of peak-predicted energy intensity over all the simulations. The data were distributed about the ideal correspondence indicating the model would neither tend to overestimate nor underestimate the location of the melting threshold.

Discussion

The results of this model compared well with experimental results despite the simplifications and absence of secondary effects. The consistency within data sets was better than between data sets for the three conditions of beam aperture, thus we chose to present these data series separately. This may be a function of changes in the spatial intensity profile as affected by the beam aperture. This was indicated by variations in the burn patterns of the apertured vs. nonapertured multimode beam. An increasingly disturbed burn profile of the focused beam was also observed in kapton burns as smaller apertures were used. The highly multimode nature of the Nd:YAG beam generally results in a very uniform "top hat" intensity profile. Burn spots of the raw beam, when apertured, showed increasingly less of a top hat shape as smaller apertures were used. This may also explain differences seen in the range of predicted melting thresholds between the first series where no beam aperture was used and the second and third series where an aperture was used.

The effect of angle-dependent reflectivity was not included within this model for two reasons, the first being simplicity and ease of calculation. The second reason is that the effect of incident angle on laser beam energy absorption is relatively small for most angles under typical drilling and welding conditions, except for those angles nearly parallel to the joint walls (Refs. 7–9). We demonstrate this by ray tracing within tapered joint root opening, as shown in Fig. 2, where few incident reflections are at low angles, with respect to the joint groove face, due to the rapid effect of angle addition on the propagating ray. Most of the energy concentration and reflection are at near-normal angles to the groove face and located in the lower portions of the weld joint. Therefore, angle-dependent absorption effects were not considered significant enough to be included within this initial model.

The effect of polarization also was not included in this model due to an argument similar to that made above for angle-dependent reflection. That is, the effect of polarization on beam absorption, with variations of S and P wave absorption as a function of incident angle, is small at angles near normal to the surface of reflection as described in Refs. 13–15. Again, these near-normal angles are characteristic of the majority of reflections predicted by the model and are concentrated near the bottom of the joint. A recent study of angle-dependant absorption and beam scattering, in simulation, was shown to have little effect on the location of energy concentration (Ref. 16). The study of the effects of polarization is left for future study.

Since the weld width data compared well with simulation results, the effect of diffuse reflections, temperature-dependent absorption and the wide range of other effects are probably minor for these conditions. Simulation of these effects will be left for future study.

Conclusions

A simple three-dimensional geometric optical ray-tracing model was used to describe the most dominant effect of well-understood parameters. The location and magnitude of the impingement of laser energy along the wall of a tapered narrow groove V joint in alloy 304 stainless steel was modeled. Qualitative comparison between the simulated melt pattern shapes and actual laser melted regions compared well for three series of tests made under varying conditions of spot size, F number and focal point location. Quantitative comparison of approximate calculated values for the melting threshold of 304 stainless steel compared relatively well with the actual melt region fusion boundaries and the corresponding predicted energy threshold values, of 5–10 J/cm^2 for the simulation, despite being based upon simple first order effects. The results of this study indicate the model is sufficiently accurate in predicting spatial and intensity effects to be useful in design and optimization of laser weld joints for a wide variety of laser materials processing applications.

Acknowledgments

This research was funded under DOE contract No. W-7405-ENG-36. The authors wish to thank S. G. Girrens, manager of the AMIP (Advanced Manufacturing Industrial Partnership) program. In addition, we would like to acknowledge the help of A. J. Pelkington of the USAF Academy for help in performing the simulation experiments and Edward Sklar, chief optical scientist of Opticad Corp., Santa Fe, N.Mex., for consultation and model development.

References

1. Mendenhall, C. E. On the emissive power of wedge shaped cavities and their use in temperature measurements. *The Astrophysical Journal* 33(2): 91–97.

2. Minamida, K., Oikawa, M., Sugihashi, A., and Kido, M. 1992. Laser welding of metal honeycomb panel with multiple reflecting effects of high power laser beams. *Proc. LIA ICALEO*, pp. 557–564.

3. Minamida, K., *et al*. 1986. Wedge shape welding with multiple reflecting effect of high power CO_2 laser beam. *Proc. Int'l Congress on Applications of Lasers and Electro-Optics*, pp. 97–104.

4. Sepold. G., Rothe, R., and Teske, K. 1987. Laser beam pressure welding — a new technique. *Proc. Conf. Laser Advanced Material Processing LAMP '87*, pp. 151–156, High Temperature Society, Osaka, Japan.

5. Huntington, C. A., and Eager, T. W. 1983. Laser welding of aluminum and aluminum alloys. *Welding Journal* 62(4): 105-s to 107-s.

6. Fuerschbach, P. W., and MacCallum, D. O. 1995. Variation of laser energy transfer efficiency with weld pool depth. *Proceedings ICALEO '95*, 80: 497–503, LIA, Orlando, Fla.

7. Bolin, S. R. 1982. The effect of F# and beam divergence on quality of holes drilled with pulsed Nd:YAG lasers. *Proceedings ICALEO*, 31: 135–140, LIA, Orlando, Fla.

8. Grevey, D. F., and Desplats, H. 1994. Comparison of the performance obtained with a YAG laser cutting according to the source operation mode. *J. Mater. Process. Technology*, 42: 341–348.

9. Yeo, C. Y., *et al.* 1994. A technical review of the laser drilling of aerospace materials. *Journal of Materials Processing Technology* 42: 15–49.

10. Milewski, J., and Sklar, E. 1995. Modeling and validation of multiple internal reflections using ultra-narrow gap laser welding. *Proceedings of ICALEO '95*, pp. 151–156, San Diego, Calif., LIA, Orlando, Fla.

11. Milewski, J., and Sklar, E. 1996. Modelling and validation of multiple internal reflections for enhanced laser welding. *Modeling and Simulation in Materials Science and Engineering*, Institute of Physics 4: 305–322.

12. Milewski, J. 1997. Modeling and design of energy concentrating weld joints. *Proceedings of the First International Conference on Welding and Joining Science and Technology*, Madrid, Spain, ASM International, Materials Park, Ohio.

13. Arata, Y. 1986. *Plasma, Electron & Laser Beam Technology*, ASM International, Materials Park, Ohio.

14. Dawes, C. 1992. *Laser Welding*, pp. 151–161, Abington Publishing, Cambridge, England.

15. Steen, W. 1984. *Laser Materials Processing*, LIA, Orlando, Fla.

16. Milewski, J., and Mustaleski, T. 1998. Modeling of laser energy concentration in narrow gap joints. Submitted to the *Proceedings of the 5th International Conference on Trends in Welding Research*, Pine Mountain, Ga., ASM International, Materials Park, Ohio.

Papers Sought for International Laser Meeting
Abstracts Due by April 30

Orlando, Fla. — The Laser Institute of America is seeking submissions for presentations at the 18th International Congress on Applications of Lasers and Electro-Optics (ICALEO'99), which will be held November 15–18, 1999 in San Diego, Calif., USA.

ICALEO'99 is an international forum for the exchange of technical information between users of lasers in industrial, government, medical and academic settings, and the scientists, engineers and technicians developing these technologies and applications.

Papers are sought for the ICALEO'99 Laser Materials Processing Conference in the areas of aerospace, automotive, advanced machining, flexible manufacturing, advanced laser sources, diode lasers, diode-pumped lasers, gas lasers, cutting, drilling, welding, surface modification, laser optical quality, process modeling and control, rapid prototyping and sensing.

For the ICALEO'99 Laser Microfabrication Conference, papers are sought in the laser fields of medical devices, electronics and processes. Specific topics include catheters, stents, microsurgical components, implantable devices, drug delivery, sensors, interconnect structures, display devices, MEMS, surface texturing, thin film patterning, silicon machining, cutting and drilling, marking, welding and bonding, etching and deposition, ultrafast laser processing, microforming and rapid prototyping. Abstracts for both conferences are due by April 30, 1999.

Paul Christensen (Potomac Photonics, Lanham, Md.) is the general chair for ICALEO'99. Paul Denney (EWI, Columbus, Ohio), Isamu Miyamoto (Osaka Univ., Osaka, Japan) and Ken Watkins (Univ. of Liverpool, UK) serve as co-chairs for the Laser Materials Processing Conference. Raj Patel (Aradigm Corp., Hayward, Calif.) and Peter Herman (Univ. of Toronto, Toronto, Canada) are co-chairs of the Laser Microfabrication Conference.

The Laser Institute of America is the professional society dedicated to fostering lasers, laser applications and laser safety worldwide.